sciendo

ANNALS OF WEST UNIVERSITY OF TIMISOARA PHYSICS
Vol. LXVI, 2024

DOI: 10.2478/awutp-2024-0003

EFFECT OF SB ADDITION ON MECHANICAL, ELECTRONIC AND THERMODYNAMIC PROPERTIES OF INTERMETALLIC B2-NIAL: FIRST PRINCIPLES STUDY

Mohamed Amine Bouchentouf[1,*], Ahmed Abdiche[2], Djamel Ghaffor[3], Azzeddine Mokadem[4], Nabil Beloufa[5] and Samir Bekheira[6]

[1]*Faculty of Material Sciences, University of Tiaret, Tiaret, 14000 Algeria.*
[2]*Electrical Engineering Department, Faculty of Applied Science, University of Tiaret, Tiaret,14000 Algeria*
[3,4]*Laboratory of Materials (LabMat), National Polytechnic School of Oran, ENPO-Maurice AUDIN, BP 1523, El M'Naouer, 31000, Oran, Algeria*
[5]*Hydrometeorological Institute for Training and Research IHFR,Ibno-Rochd, Bp7019, Oran, Algeria.*
[6]*Laboratory of Micro and Nanophysics (LaMiN), National Polytechnic of School Oran, ENPO-Maurice AUDIN, BP 1523, El M'Naouer, 31000, Oran, Algeria*
**Corresponding author: Email: aminebouchentouf12@gmail.com*

Article Info

Received: 22.12.2023
Accepted: 22.02.2024

Keywords:

FP-LAPW, Mechanical properties, $NiAl_{1-x}Sb_x$,GGA, Ductility

Abstract

This study investigates the mechanical, electronic, and thermodynamic properties of B2 NiAl alloyed with Sb, ranging from 0% to 100%. The calculations were conducted using the WIEN2k code based on the full potential linearized augmented plane wave (FP-LAPW) method within the density functional theory (DFT) framework. Generalized Gradient Approximation (GGA) was employed to approximate the exchange-correlation energy. Our analysis of formation enthalpy indicates a preference for Sb to substitute Al sites. Furthermore, we have observed that the mechanical properties of NiAl can be enhanced by adjusting the chemical composition of Sb. Specifically, an increase in antimony content from 0% to 75% results in a notable improvement in ductility tensile, elevating it from 1.92 to 10.72. Conversely, this alteration diminishes the material's strength.

Moreover, both the band structures and density of states (DOS) indicate the metallic behavior exhibited by all $NiAl_{1-x}Sb_x$ compounds. In addition, we employ the Gibbs2 code to calculate thermodynamic properties, shedding light on the influence of temperature and pressure on the volume, heat capacity, Debye temperature and entropy S of $NiAl_{1-x}Sb_x$.

1. Introduction

Intermetallic alloys are compounds that comprises two or more metallic elements, possibly with one or more non-metals, and possesses a crystal structure distinct from those of its constituent elements [1]. A substantial number of these compounds exhibit stability in the B2-type and CsCl (space group 221_pm-3m) crystal structures. Given their superior ductility and lower specific gravity, the B2 structured compounds seem more favorable for aerospace applications compared to those structured differently [2].

The incorporation of aluminum into intermetallic alloys holds significant importance due to its ability to confer a range of advantageous properties. Aluminum's contribution to enhanced creep resistance, mechanical properties, and thermal conductivity further extends their utility [3]. These alloys such as : Al-Ni, Al-Ti and Al-Fe exhibit a combination of lightweight strength, high-temperature stability, corrosion and oxidation resistance, making them valuable in aerospace, automotive, and high-temperature applications

One notable intermetallic alloy is NiAl, which exhibits impressive properties such as : high melting point, excellent corrosion-resistant, low density and high thermal conductivity [4, 5], rendering it suitable for high temperature application [6, 7], particularly in aircraft gas turbine blades [8, 9]

During the past years, there has been extensive research dedicated to examining NiAl-based intermetallics, primarily focusing on enhancing their mechanical properties. These investigations center around the incorporation of alloying elements to enhance ductility, especially at lower temperatures—a crucial factor in designing materials and devices [9]. These endeavors aim to broaden the potential scope of applications for these materials. Ab initio calculations have played a pivotal role in numerous studies that delve into the influence of various alloying elements on the mechanical properties of NiAl-based alloys. Noteworthy among these contributions, P. Lazar and R. Podloucky [10] concentrated on microalloying NiAl with X=Cr, Mo, Ti, and Ga, uncovering the significant potential of Cr and Mo in augmenting the ductility of NiAl-X alloys. Similarly, Jun-Qi He et al. [11] delved into rare earth microalloying elements (Sc, Y, La, and Nd), highlighting the ductility improvement brought about by all four elements, with Ni_8Al_7La emerging as exceptionally ductile. Expanding upon this line of inquiry, Ponomareva et al. [12] explored NiAl-based systems alloyed with Sc, Ti, V, Cr, W, Re, and Co, projecting enhanced ductility with the introduction of W, V, Ti, and Re into B2-NiAl. In another work [13] the same authors, specifically examined the influence of rhenium content, noting increased alloy ductility for Re fractions surpassing 30 at.%. In contrast, Yong Cao et al. [14] investigated Co-alloyed NiAl, uncovering decreased

alloy plasticity as indicated by B/G and υ values. Investigating Cr and V alloying, S. Yalameha and A. Vaez [15] observed reduced ductility compared to that of NiAl. Furthermore, Wenjie Chen et al. [16] studied the effects of alloying elements Ru, Rh, Os, and Ir, demonstrating heightened ductility in NiAl. Reflecting on ternary elements (Fe, Co, Mo, W, Pt, Sc, and Y) and their incorporation into B2 NiAl, H. Hu et al. [17] revealed the collective effectiveness of these elements in enhancing ductility. Together, these comprehensive studies underscore the potential to tailor NiAl-based alloy mechanical properties through strategic alloying to achieve improved ductility.

Recent advancements have demonstrated the enhancement of both ductility and strength in high-entropy alloys by introducing metalloid elements. These elements possess properties that bridge the gap between metals and nonmetals [18]. Our idea involves incorporating a substantial amount of the metalloid element antimony (Sb) into NiAl in order to enhance the ductility, particularly at lower temperatures. Notably, there have been no prior investigations into the mechanical effects of different Sb additions on NiAl compounds. Building upon this premise, we conducted an investigation encompassing seven sets of $NiAl_{1-x}Sb_x$ (x = 0.125; 0.250; 0.375; 0.50; 0.625; 0.750; 0.875; 1.0) alloys, utilizing the FP-LAPW method.

The paper comprises three main sections. The initial part offers a broad introduction, while the subsequent one delves into various methodologies used to compute the physical properties of the material. The third section details the attained results and their corresponding interpretations. Finally, the study culminates with a comprehensive conclusion summarizing our findings.

2. Computational method

In this study, we have used the density functional theory (DFT) based on the full potential linearized augmented plane wave (FP-LAPW) method as implemented in WIEN2k [19] to calculate the structural, mechanical, electronic and thermodynamic properties of $NiAl_{1-x}Sb_x$ alloys, where the value of x ranges between 0 and 1, exhibiting increments of 0.125. The Perdew-Burke-Ernzerhof (PBE) parameterization of the generalized gradient approximation (GGA) [20]. A 10x10x10 k-point mesh was utilized in the irreducible wedge of the Brillouin zone (IBZ) to ensure energy convergence, with muffin-tin spheres of radius 1.92 and 2.20 atomic units (a.u.) for Ni and Sb atoms, respectively, and a value of 1.66 a.u. for Al atoms. The maximum value for wave function expansion within spheres was set to l_max = 10, and the plane wave cutoff of k_max = 8/RMT was limited for the expansion of wave functions in the interstitial region, where RMT is the smallest atomic sphere radius inside the cell and k_max

is a cutoff for the basis function wave vector. The charge density was Fourier-expanded up to G_max = 12 (a.u.).

A supercell measuring 2x2x2 was generated from the B2-NiAl unit cell, comprising Al cations positioned at (0,0,0) and Ni anions at (0.5;0.5;0.5). This enlargement resulted in a unit cell housing 16 atoms. Subsequently, we replaced one, two, three, four, five, six, and seven atoms of either Ni or Al with Sb, forming compounds with compositions of 12.5%, 25%, 37.5%, 50%, 62.5%, 75%, and 87.5%.

3. Results and discussions

3.1. Site preference of Sb addition to B2-NiAl at ground state

First we compute the total energy as a function of the unit cell volume for all NiAl compounds that have been alloyed with Sb. This investigation covers two scenarios: one where Sb replaces Ni atoms, and another where Sb takes the place of Al atoms.

To determine the site preference of the Sb additions in *B*2 NiAl at $T = 0$ K (Al site or Ni site), we calculate the difference between the formation enthalpies (transfer energy E_T) of $AlNi_{1-x}Sb_x$ and $NiAl_{1-x}Sb_x$ [21, 22] as following :

Formation enthalpy of Ni atom replaced by Sb can be given by:

$$\Delta H_{Ni} = E(AlNi_{1-x}Sb_x) - (1-x)E_{Ni} - xE_{Sb} \quad (1)$$

While formation enthalpy of Al atom replaced by Sb as follows:

$$\Delta H_{Al} = E(NiAl_{1-x}Sb_x) - (1-x)E_{Al} - xE_{Sb} \quad (2)$$

Here, we define $E(AlNi_{1-x}Sb_x)$ and $E(NiAl_{1-x}Sb_x)$ as the total energies (plotted in Figure1(a-i)) associated with the introduction of ternary element Sb to replace the Ni and Al sublattices, respectively. Additionally, E_{Ni}, E_{Al}, and E_{Sb} represent the average total energies of individual atoms in their bulk states. The transfer energy, denoted as E_T ($E_T = \Delta H_{Ni} - \Delta H_{Al}$), serves as a crucial metric for determining site preference behaviors, if $E_T < 0$, it indicates a strong preference for the Ni site, whereas if E_T is greater than or equal to zero, it signifies a preference for the Al site.

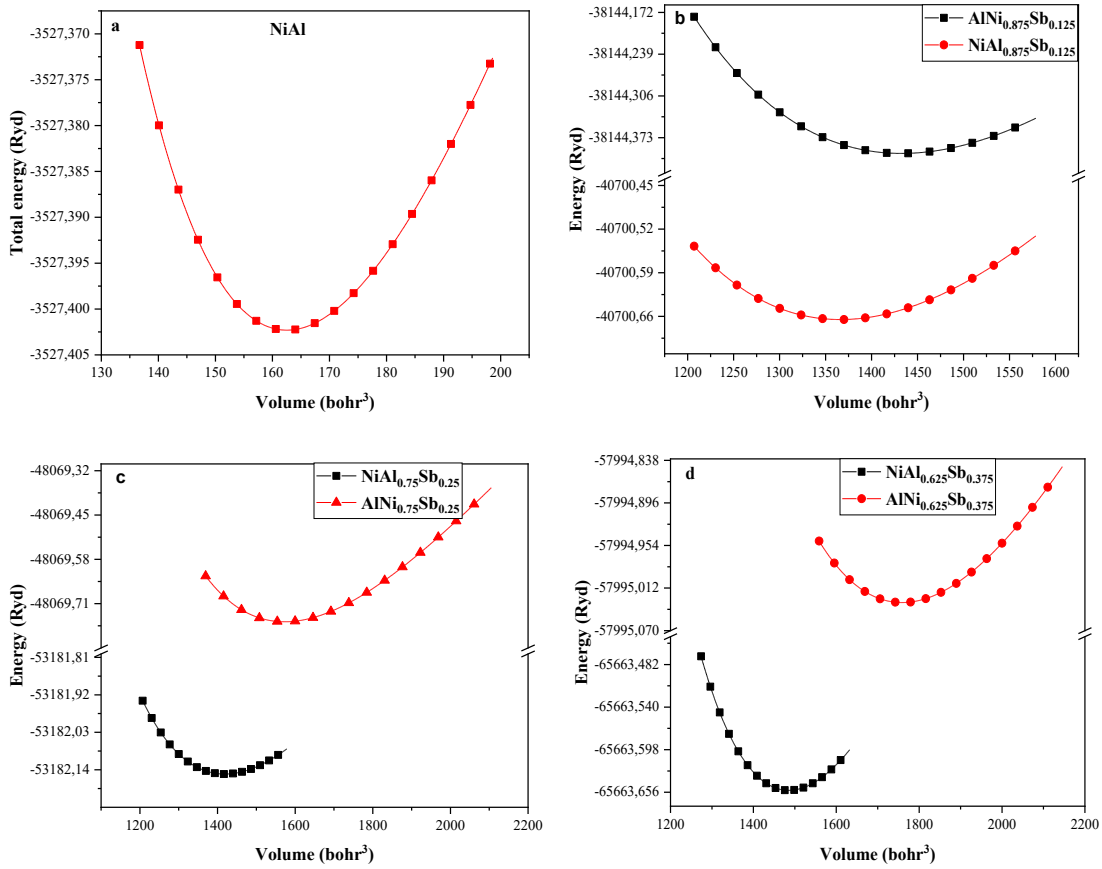
In Figure 1 (a-i), we proved that the Sb atoms could be alloyed to the binary compound NiAl to form the ternary $NiAl_xSb_{1-x}$. Henceforth, we found that Sb atoms substitute to Al atoms

preferentially as shown in Table 1. Table 1 also presents the computed structural parameters in the ground equilibrium states, which were determined by fitting the total energy curves to the Birch-Murnaghan's equation of state [23]. One can see that the bulk modulus decrease with increasing of Sb composition which can result in lower hardness.

To the best of our knowledge no experimental or theoretical findings regarding the properties of $NiAl_{1-x}Sb_x$ ternary compounds have been previously reported, and as a result, the outcomes acquired in this study may help fill the knowledge gap in the literature concerning these ternary alloys.

Table 1. Transfer energy E_T and site preference of Sb ternary element in B2 NiAl with calculated lattice constants and bulk modulus of resulted compounds

Sb composition	H_{Ni} (eV)	H_{Al} (eV)	Transfer energy (E_T)	Site preference	a_0 (Å)	B_0 (GPa)
0%	/	/	/	/	2.892	155.67
12.5%	-10.32	-14.08	3.76	Al	2.935	152.18
25%	-8.07	-13.64	5.57	Al	2.973	148
37.5%	-5.15	-13.40	8.25	Al	3.018	133.45
50%	-4.99	-12.79	7.80	Al	3.083	120
62.5%	-4.54	12.99	8.45	Al	3.132	118.52
75%	-7.16	-13.53	6.37	Al	3.179	116
87.5%	-8.62	-14.42	5.80	Al	3.220	115.48
100%	/	/	/	/	3.252	109.0



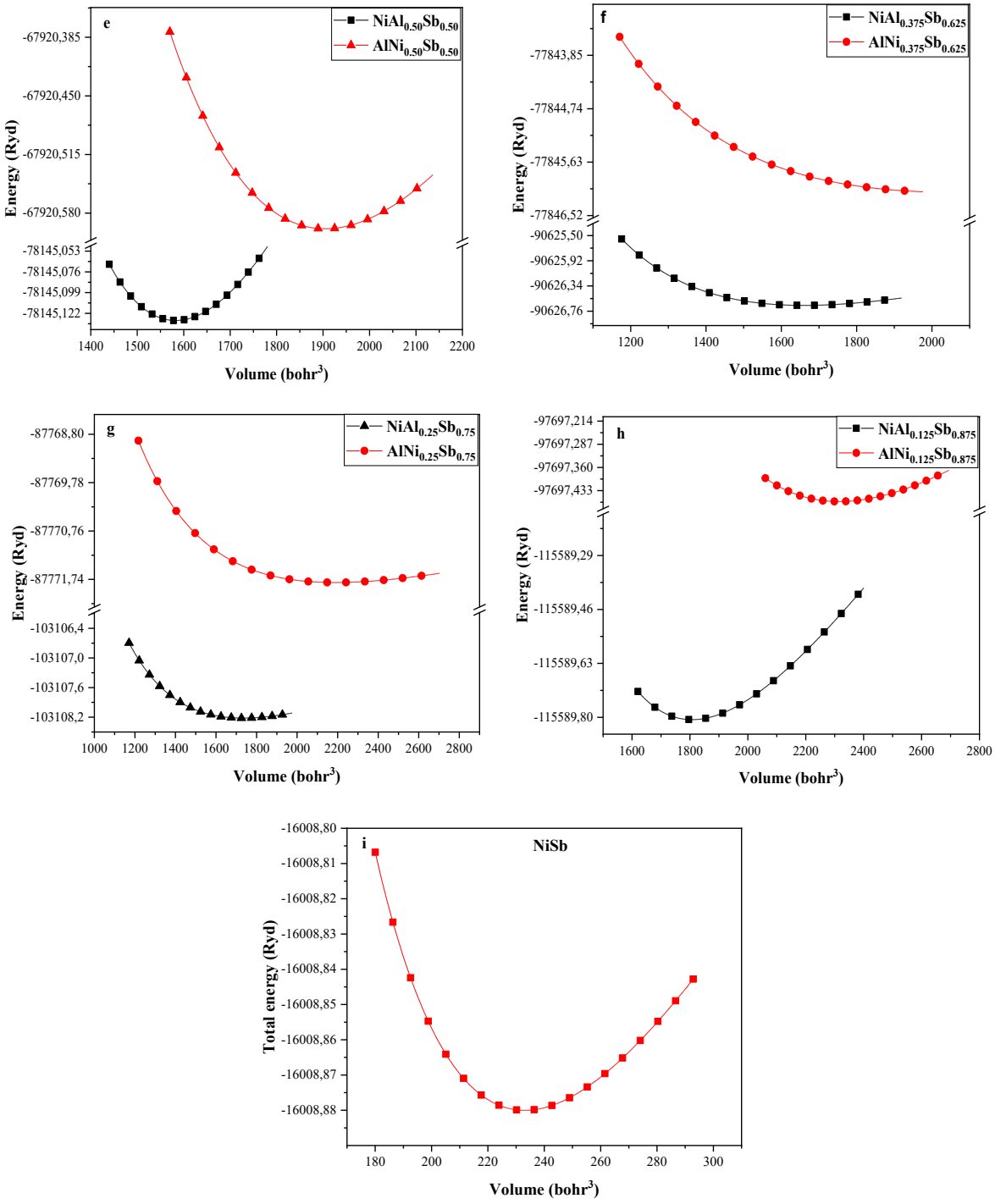


Figure 1. (a-i) Total energy versus volume unit cell of $NiAl_{1-x}Sb_x$ and $AlNi_{1-x}Sb_x$

3.2. Mechanical properties

Using the IRelast package [24] implemented in Wien2k, we examine how the introduction of Sb effects on the mechanical properties of B2-NiAl, we computed the elastic constants (C_{11}, C_{12}, and C_{44}) related to the cubic structure for the compounds under investigation.

The results obtained for NiAl, as shown in Table 2, exhibit en general good concurrence with prior experimental findings and theoretical computations, thereby validating the accuracy of our calculations.

In accordance with the Born stability criteria, mechanical stability must satisfy the following conditions [25]*:*

$$C_{11} - C_{12} > 0,\ C_{11} > 0,\ C_{44} > 0,\ C_{11} > |C_{12}|,\ (C_{11} + 2C_{12}) > 0 \quad (3)$$

In light of these criteria, the examined compounds are mechanically stable. Table 2 includes also the values of the other mechanical quantities,*i.e*: bulk modulus (B), Young modulus (E) and shear modulus (G) that are obtained as following:

$$B = \frac{C_{11}+2C_{12}}{3} \quad (4)$$

$$E = \frac{9BG}{3B+G} \quad (5)$$

$$G = \frac{G_V+G_R}{2} \quad (6)$$

Where $G_V = (C_{11} - C_{12} + 3C_{44})/5$ is the Voigt shear modulus corresponding to the upper bound of G value and $G_R = 5(C_{11} - C_{12})C_{44}/[4C_{44} + 3(C_{11} - C_{12})]$ is the Reuss shear modulus conforming to the lower bound of G value.

It is important to highlight that no reports on mechanical parameters of $NiAl_xSb_{1-x}$ ternary compounds are available, making it currently unfeasible to draw comparisons with other materials. Nonetheless, it is noteworthy that the calculated bulk modulus as plotted in Figure 2, derived from elastic constants, exhibits a high level of agreement with the value obtained from total energy minimization. This convergence offers insight into the potential reliability and accuracy of our predicted elastic constants for the $NiAl_{1-x}Sb_x$ compounds. Also, As the concentration of Sb increases, the bulk modulus decreases. A notable observation is that the bulk modulus in NiAl is higher than in $NiAl_{1-x}Sb_x$, primarily due to the bond nature. The covalent bond between Ni and Al is stronger than the metallic bond between Ni and Sb, contributing to this difference in bulk modulus.

Figure 3 illustrates how the elastic constants change relative to the composition (x) of the $NiAl_{1-x}Sb_x$ compounds. The graph clearly demonstrates that as x increases, the elastic constants

consistently decrease in all dimensions. This decreasing can be attributed to the expansion of the anionic radius. As a result, it can be inferred that the elastic constants decrease as the crystal lattice parameter expands. This phenomenon was observed by Carlos et al [26].

Additionally, in Figure 4, we have graphed the variations in shear and Young moduli following the composition (x) of $NiAl_{1-x}Sb_x$. It becomes evident that the shear and Young moduli of the $NiAl_{1-x}Sb_x$ ternary compounds decrease as x composition increases. This trend can be rationalized by the fact that the incorporation of Sb weakens the chemical bonds due the formation of metallic bonds between Sb and Ni.

Both the ratio of the bulk modulus to the shear modulus (*i.e* the B/G ratio) and Pugh's criterion [27] has been employed and illustrated in Figure 5 as functions of composition x for the $NiAl_{1-x}Sb_x$ ternary alloys to classify the material's characteristics as either ductile or brittle. A material is considered ductile if its B/G ratio surpasses 1.75, while it is categorized as brittle if it falls below this threshold. Analysis of the data reveals that all the compounds exhibit a higher degree of tensile ductility between 1.90 and 10.72. These findings underscore the notable alloying effects associated with the Sb addition. Furthermore, the variations in the B/G ratio are mirrored by analogous trends in Poisson ratio with respect to composition x, thus reinforcing the assessment of ductile behavior in the $NiAl_{1-x}Sb_x$ alloys.

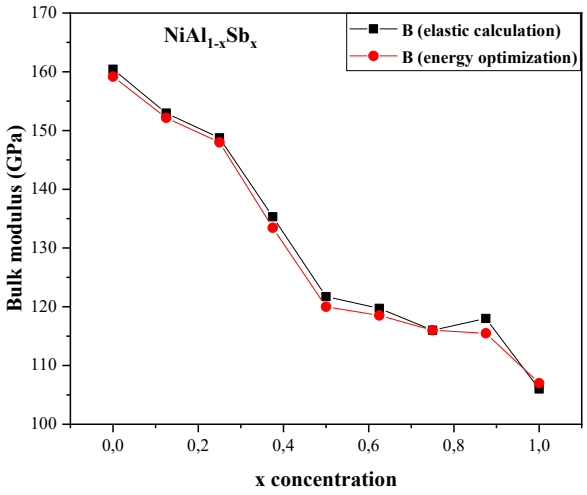


Figure 2. Variation of bulk modulus B (GPa) in function of x concentration of $NiAl_{1-x}Sb_x$ compounds

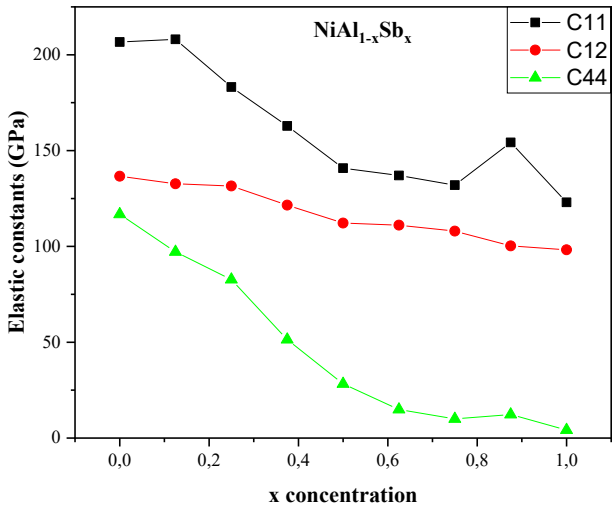


Figure 3. Variation of elastic constants in function of x concentration of $NiAl_{1-x}Sb_x$ compounds

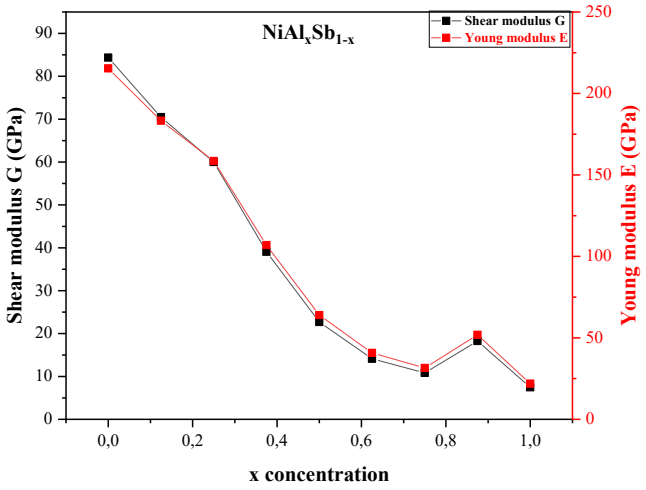


Figure 4. Variation of Shear modulus and Young modulus in function of x concentration of $NiAl_{1-x}Sb_x$ compounds

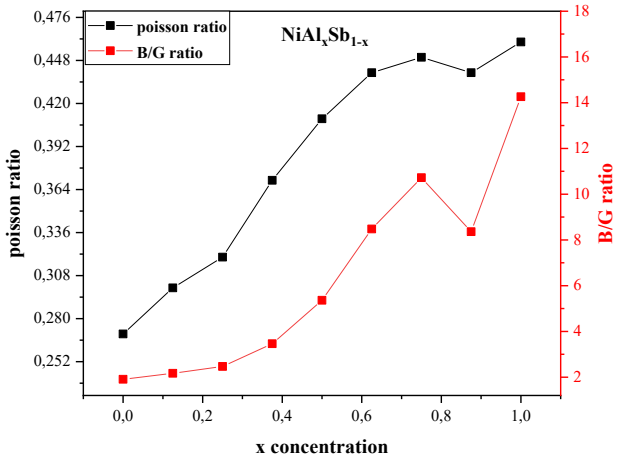


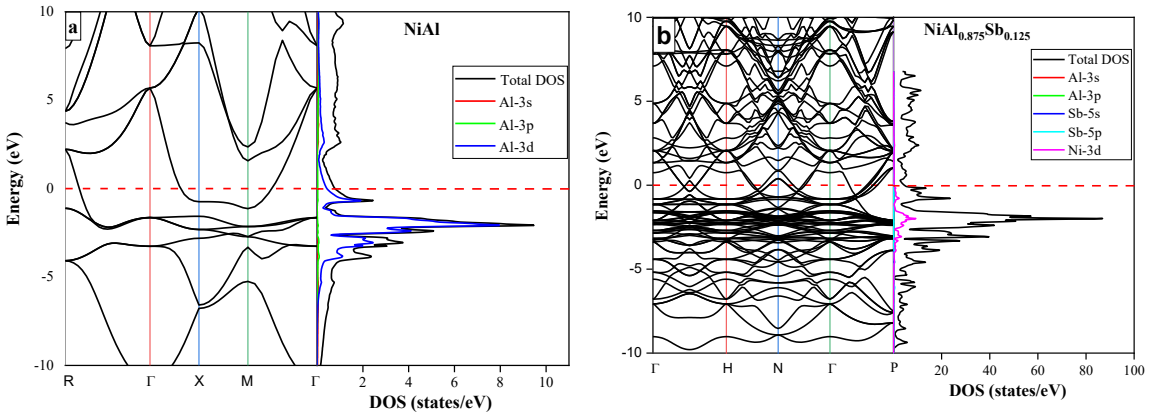
Figure 5. Variation of B/G ratio and Poisson ratio **ν** in function of x concentration of $NiAl_{1-x}Sb_x$ compounds

Table 2: Calculated of elastic constants (C_{11}, C_{12} and C_{44}), Bulk modulus (B), Young Modulus (E), Shear modulus (G), B/G ratio, poisson ratio (ρ ratio) and Cauchy pressure (C_{11}-C_{44}) of $NiAl_{1-x}Sb_x$

Compounds	C_{11} (GPa)	C_{12} (GPa)	C_{44} (GPa)	B (GPa)	E (GPa)	G (GPa)	B/G	ρ ratio	C_{11}-C_{44} (GPa)
NiAl (our work) Other theory [28] Experiment [29]	206.64 203.14 204.6	136.62 131.69 135.4	116.78 112 116.8	160.44 155.51 158.5	215.3	84.36	1.90	0.27	89.86
$NiAl_{0.875}Sb_{0.125}$	208.07	132.68	97.18	152.97	183.28	70.47	2.17	0.30	96.35
$NiAl_{0.75}Sb_{0.25}$	183.15	131.55	82.71	148.75	158.5	60	2.47	0.32	100.44
$NiAl_{0.625}Sb_{0.375}$	162.83	121.57	51.36	135.32	106.9	39.07	3.46	0.37	111.47
$NiAl_{0.50}Sb_{0.50}$	140.82	112.18	28.29	121.73	64	22.7	5.36	0.41	112.53
$NiAl_{0.375}Sb_{0.625}$	137	111.11	14.91	119.73	40.75	14.12	8.48	0.44	122
$NiAl_{0.25}Sb_{0.75}$	132	108	10	116	31.50	10.82	10.72	0.45	122
$NiAl_{0.125}Sb_{0.875}$	135.03	99.49	9.66	111.34	37.28	12.90	8.63	0.44	125.37
NiSb	123.01	98.25	4.19	106.51	21.88	7.46	14.27	0.46	118.82

3.3. Electronic properties

In one plot, Figure 6 (a-i) displays both the calculated total and partial density of states alongside the band structure where the first Brillouin zone is represented with the high symmetry directions of NiAl and $NiAl_{1-x}Sb_x$ at zero pressure. Accordingly, the red dash line represents the fermi level. After alloying, small changes were observed in the total and partial density of states (TDOS and PDOS) for Ni and Al. As depicted in figure 6, the band structure at the Fermi energy remains non-zero, suggesting that the considered compounds are metallic. The dominant contribution near the Fermi level in the valence band region of all compounds stems from the d-orbitals of Ni, with a secondary contribution originating from the p-orbitals of Sb atoms. Despite this, there is still another smaller observed contribution coming from the sp-orbitals electrons of Al in this region.



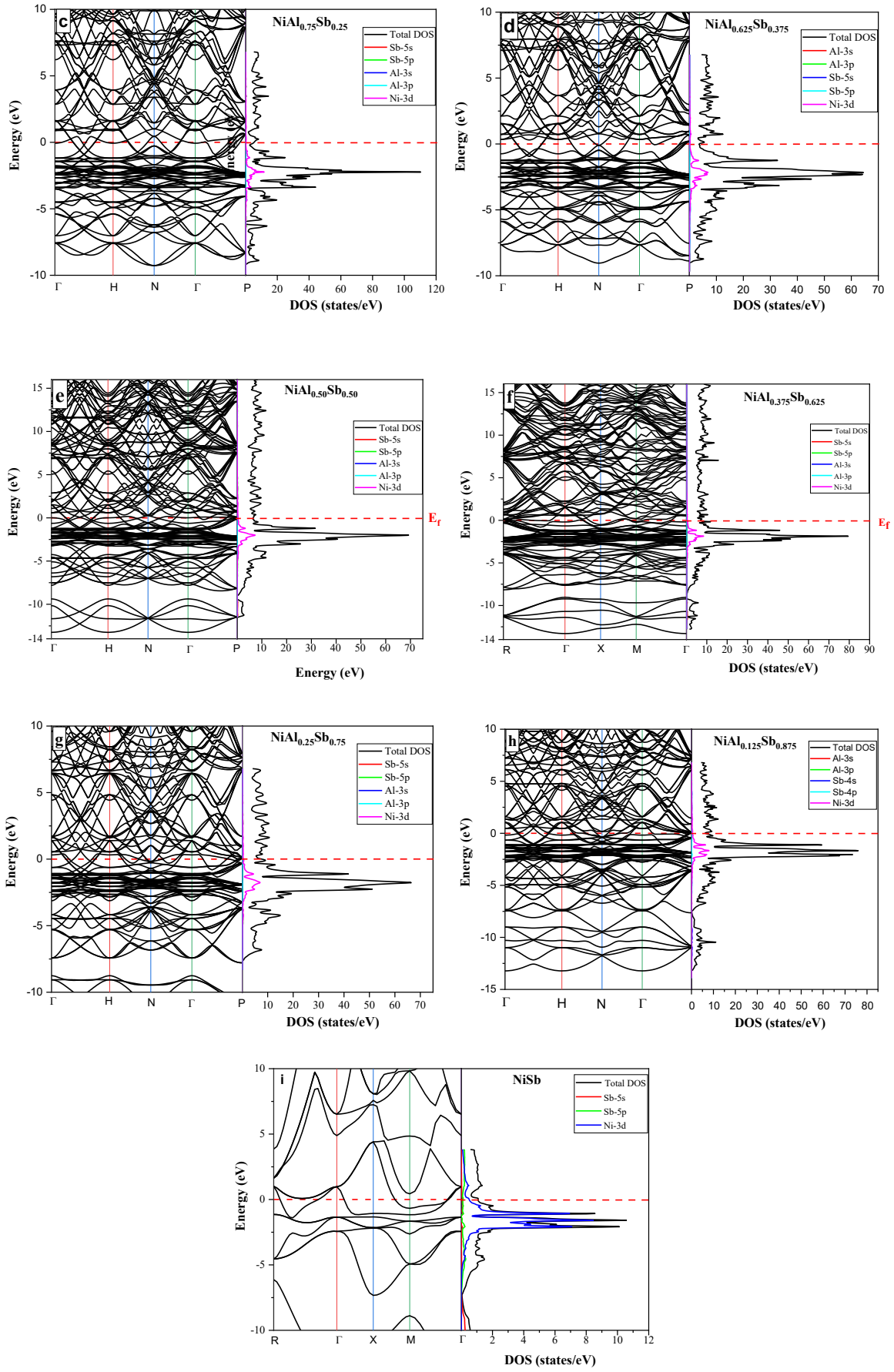


Fig. 6 (a-i). The band structures and density of states of $NiAl_{1-x}Sb_x$ compounds

3.4. Thermodynamic properties

In our exploration of the effect of temperature and pressure on $NiAl_{1-x}Sb_x$ compounds, we engage in the computation of thermodynamic properties. Specifically, we assess variations in Volume, heat capacity, Debye temperature and entropy. This analysis is conducted employing the Gibbs program [30] and is grounded in the Quasi-Harmonic Debye model. For a more comprehensive insight into the calculations, we direct the reader to consult the work by Httabi et al [31] and the references cited therein. Our investigation spans a temperature range of 0 to 3000 K and a pressure range of 0 to 40 GPa with the step of 8 GPa.

Figure 7 (a-i) illustrates the relationship between the volume of $NiAl_{1-x}Sb_x$ and its temperature under different fixed pressures. Notably, the volume undergoes a substantial expansion as temperature increases. This phenomenon is primarily due to the heightened thermal motion of the constituent particles within the compounds as temperature rises, leading to a swift volume increase. Conversely, a significant volume reduction occurs with an increase in pressure. This reduction can be ascribed to compression of unit cell dimensions, resulting in a more compact structure.

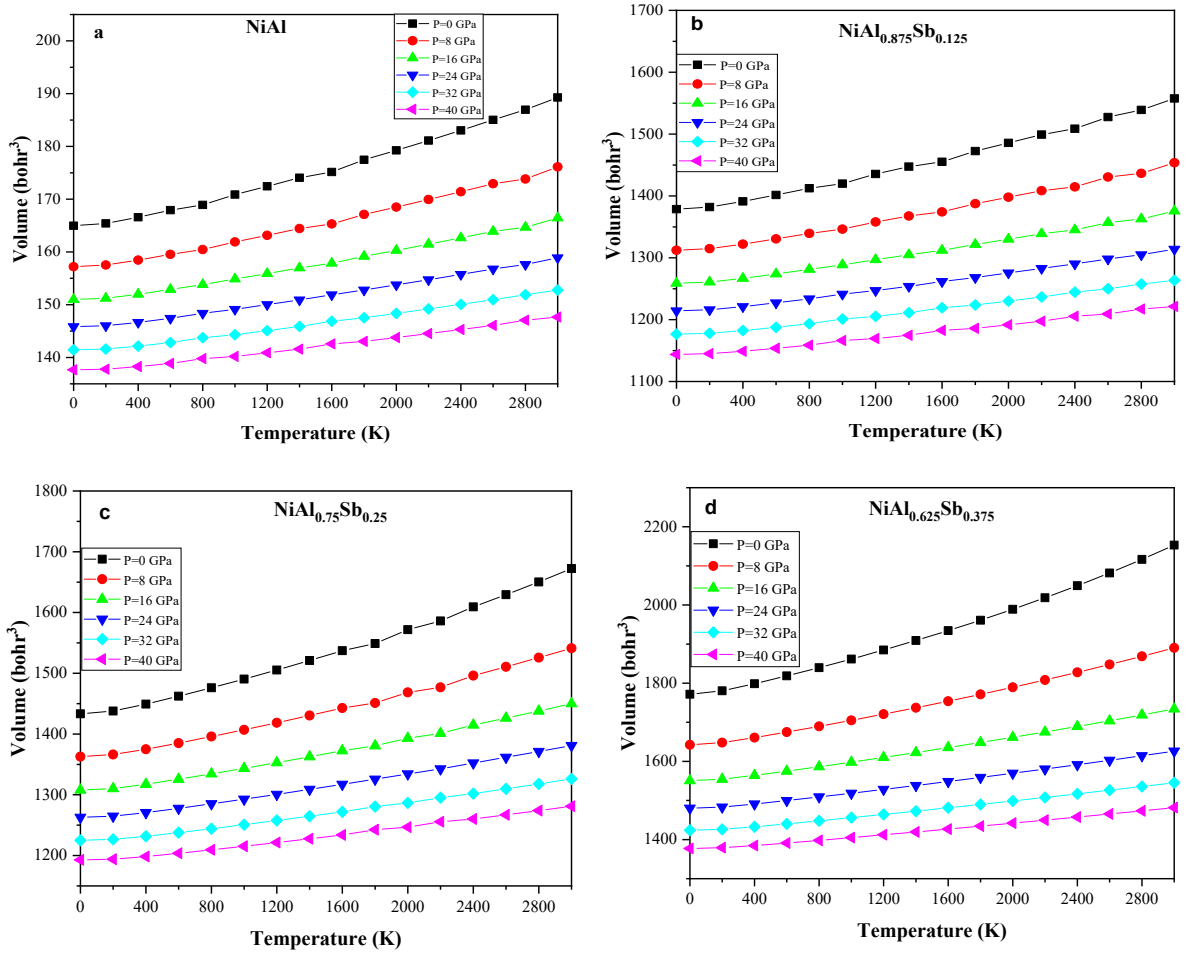
Figure 8 (a-i) depicts the variations of heat capacity $\mathbf{C_v}$ concerning temperature at various pressures for $NiAl_{1-x}Sb_x$ alloys. At low temperatures, the evident proportionality of heat capacity to $\mathbf{T^3}$ aligns with the predictions of the Debye model. As temperature rises, $\mathbf{C_v}$ undergoes a rapid increase owing to heightened anharmonic effects, while at higher temperatures, it approaches the classical Dulong–Petit limit, indicating the excitation of all phonon modes. Moreover, at a given pressure, $\mathbf{C_v}$ demonstrates an increase with rising temperature and a slight decrease with increasing pressure at a given temperature.

The Debye temperature stands as a significant characteristic temperature for solids. As the temperature increases from absolute zero, the solid's atoms progressively undergo vibrational motion until they reach the Debye temperature. This temperature marks the point at which these vibrations attain their maximum possible modes. It serves as a useful approximation for the hardness of solids. Figure 9 (a-i) shows the Debye temperature θ_D as function of temperature, respectively for $NiAl_{1-x}Sb_x$ at different pressures. At a given pressure, Debye temperature θ_D is found to be nearly constant from 0 K to 100 K. At high pressures, the Debye temperature increases with pressure when the temperature is fixed, this is due to the hardness of these materials. However, at constant temperature and pressure, the Debye temperature gradually decreases following the order: $NiAl > NiAl_{0.875}Sb_{0.125} > NiAl_{0.75}Sb_{0.25} > NiAl_{0.625}Sb_{0.375} > NiAl_{0.50}Sb_{0.50} > NiAl_{0.375}Sb_{0.625} > NiAl_{0.25}Sb_{0.75} > NiAl_{0.125}Sb_{0.875} > NiSb$. This sequence implies that NiAl possesses stronger interatomic forces and superior stiffness

compared to the other compositions. This distinction is attributed to the weakening of bonds between Ni and Al caused by the presence of Sb in the alloy.

The entropy S of compound can be defined as a measure of disorder of a system in microscopic scale. The calculated entropy (S) of $NiAl_{1-x}Sb_x$ compounds are shown in figure 10 (a-i) Under normal conditions, the entropy values for NiAl, NiSb, and $NiAl_{1-x}Sb_x$ are 65.039, 48.24, and 241.61 $J.mol^{-1}.K^{-1}$, respectively. It's evident that entropy non-linearly increases with rising temperature and decreases as pressure escalates. Notably, the decline in entropy with increasing pressure slows down as temperature rises. The ternary alloy's entropy, obtained by blending NiAl and NiSb binaries, notably surpasses the individual binary compounds. This is anticipated as mixing typically introduces disorder, increasing the potential microstates and consequently, the entropy. As pressure increases, its impact on entropy diminishes gradually, and the absolute value of entropy decreases. This can be understood by considering that heightened pressures stiffen the crystal structure, reducing the number of phonon modes at any given temperature due to decreased atomic vibrations' amplitudes.

As far as we are aware, there exists no other theoretical or experimental data available for comparison with the findings presented in this study.



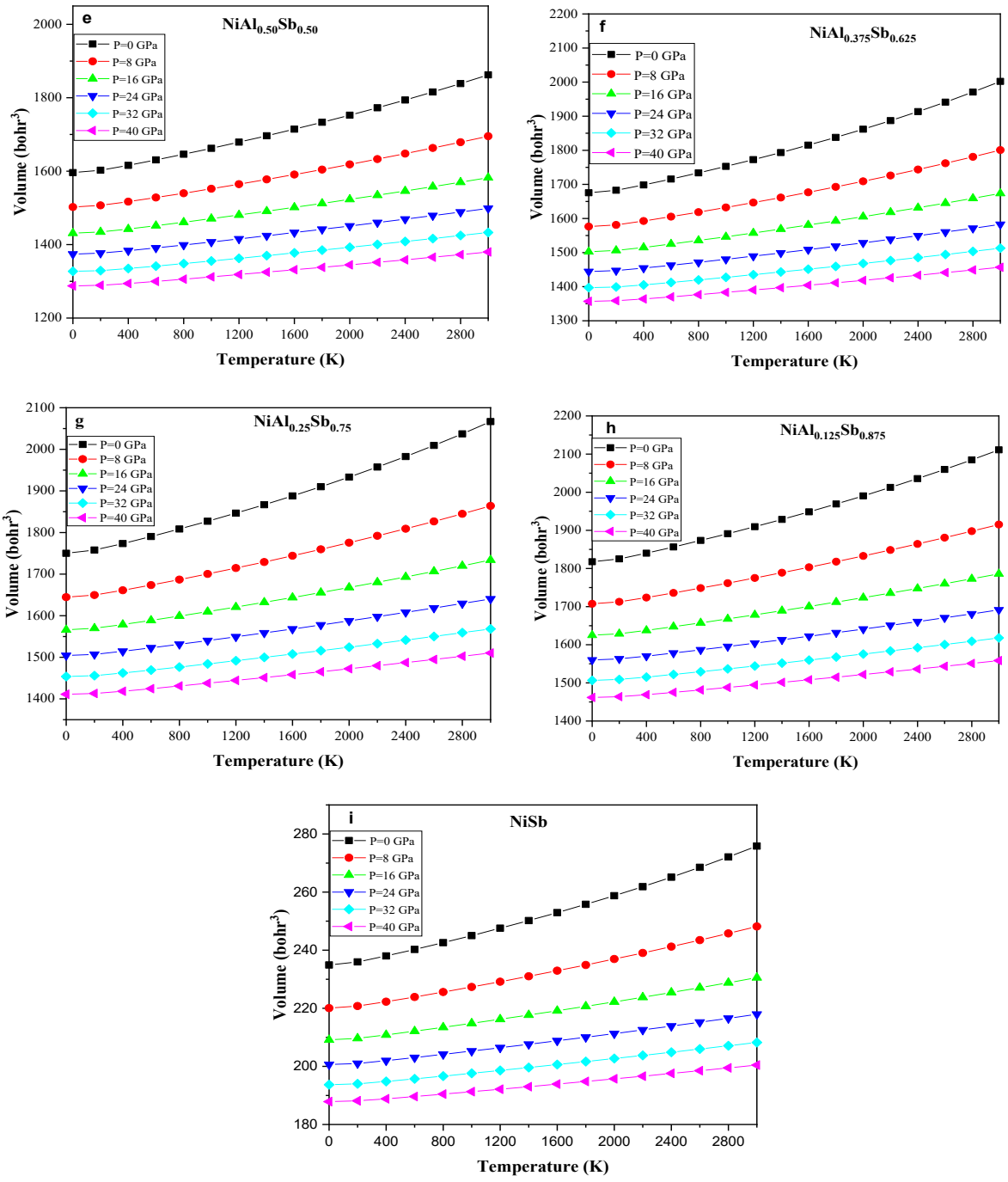


Figure 7 (a-i). Variation of volume for $NiAl_{1-x}Sb_x$ ($0<x<1$) versus temperature under different pressure

The main objective of this study was to carry out a research on the mechanical, electronic and thermodynamic properties of the NiAl-systems and to explore the impact of microalloying Sb metalloid with regard to its uses in some demanding high-tech domains. To reach this, Ab initio Density Functional Theory (DFT) calculations were conducted. As first result, we proved that the Sb exhibits a preference for substituting Al sites within the NiAl structure. So, the

introduction of Sb leads to an increase in the lattice constant of NiAl while concurrently decreasing the bulk modulus.

To get deeper insights on the mechanical properties of the $NiAl_{1-x}Sb_x$ compounds, a set of mechanical parameters was chosen (*i.e.* bulk, Young and shear moduli) and studied as a function of the Sb-concentration. It appears, using these parameters with the Pough's Criterion that the ductility-brittle balance was carefully investigated. The compounds' ductility is enhanced by the addition of Sb, up to a maximum of 75%, but this improvement is accompanied by a reduction in strength. However, the challenge of simultaneously enhancing both ductility and strength, achieving a harmonious balance of high strength and high ductility, still remains an unanswered question.

Additionally, the study delved into temperature and pressure-dependent thermal properties using the quasi-harmonic approximation. This thermodynamical analysis provided insights into the variations of volume, heat capacity, Debye temperature and entropy S across a temperature range spanning from 0 to 3000 K with a step of 200 K, at different fixed pressures rising from 0 to 40 GPa with a step of 8 GPa. We found that the properties of the studied materials are enhanced compared with those of the pure NiAl in that sense the mechanical properties are preserved as well.

References

[1] A.R. Paul, M. Mukherjee, D. Singh, *Crystal research and technology*, 57(3) (2022) 2100159

[2] R. L. Fleischer, *Platinum Metals Review*, 36(3) (1992) 138

[3] W. Miller, L. Zhuang, J. Bottema, A. J. Wittebrood, P. De Smet, A. Haszler, and A. Vieregge, *Materials Science and Engineering: A*, 280(1) (2000) 37

[4] G. K. Dey, *Sadhana*, 28 (2003) 247

[5] H. Grabke, *Intermetallics*, 7(10) (1999) 1153

[6] E. Busso, F.A. McClintock, *Acta metallurgica et materialia*, 42(10) (1994) 3263

[7] R. Darolia, *JoM*, 43 (1991) 44

[8] P. Schilke, *Advanced gas turbine materials and coatings.* GE Energy, 2004

[9] T. Yang, B.X. Cao, T.L. Zhang, Y.L. Zhao, W.H. Liu, H.J. Kong, J.H. Luan, J.J. Kai, W. Kuo and C.T. Liu, Materials today, 52 (2022) 161

[10] P. Lazar and R. Podloucky, *Physical Review* B, 73(10) (2006) 104114

[11] J.-Q. He, Y. Wang, M.-F. Yan, Y. Yang, and L. Wang, *Computational materials science*, 50(2) (2010) 545

[12] A. Ponomareva, E. Isaev, Y. K. Vekilov, and I. Abrikosov, *Physical Review B*, 85(14) (2012) 144117

[13] A. Ponomareva, Y. K. Vekilov, and I. Abrikosov, *Journal of alloys and compounds*, 586(10) (2014) S274

[14] Y. Cao, P. Zhu, J. Zhu, and Y. Liu,*Computational Materials Science*, 2016. 111: p. 34-40. 111 (2016) 34

[15] S. Yalameha and A. Vaez,*Computational Condensed Matter*, 21 (2019) e00415

[16] W.Chen, L. Xinmei and L. Caibin, College of Mechanical Engineering, Xinjiang University, Urumqi 830000, China (2023) 17

[17] H. Hu, S. Li, Y. Ren, W. Liu, and H. Zhao, *Physica B: Condensed Matter*, 576 (2020) 411703

[18] D. Wei, L. Wang, Y. Zhang, W. Gong, T. Tsuru, I. Lobzenko, J. Jiang, S. Harjo, T. Kawasaki, and J. W. Bae, *Acta Materialia*, 225 (2022) 117571

[19] K. Schwarz and P. Blaha, *Computational Materials Science*, 28 (2) (2003) 259

[20] J. P. Perdew, K. Burke, M. Ernzerhof, *Physical Review Letter,* 77(18) (1996) 3865

[21] X. Hao, P. Jia, Y. Cui, J. Wang, F. Gao, and Y. Qiao, *Journal of Alloys and Compounds*, 658(2016) 1025

[22] W. Wolf, R. Podloucky, P. Rogl, and H. Erschbaumer, Intermetallics, 4 (3) (1996) 201

[23] F. D. Murnaghan, *Proceedings of the National Academy of Sciences*, 90(9) (1944) 244

[24] M. Jamal, M. Bilal, I. Ahmad, and S. Jalali-Asadabadi, *Journal of Alloys and Compounds*, 735) (2018) 569

[25] M. Born, K. Huang, M. Lax, *American Journal of Physics*, 23(7) (1955) 474.

[26] C. M. O. Bastos, F. P. Sabino, G. M. Sipahi, and J. L. F. Da Silva*, Journal of Applied Physics*, 123(6) (2018)

[27] S. F. Pugh, *The London, Edinburgh, and Dublin Philosophical Magazine and Journal of Science*, 45(367) (1954) 823

[28] L. Liu, X. Wu, R. Wang, W. Li, Q. Liu, *Computational Materials Science*, 103 (2015) 116

[29] D. Farkas, B. Mutasa, C. Vailhe, and K. Ternes, *Modelling and Simulation in Materials Science and Engineering,* 1995. 3(2): p. 201. 3(2) (1995) 201

[30] A. Otero-de-la-Roza, V. Luaña, *Computer Physics Communications*, 182(8) (2011) 1708

[31] I. Hattabi, A. Abdiche, S. Naqib, and R. Khenata, *Chinese Journal of Physics*, **59** (2019) 449